5N THRUSTER THERMO-ELASTIC ANALYSIS

José Ricardo Soria Porro
FIBRAFORTE Engenharia Ind. Com. Ltda
ricardo.soria@fibraforte.com.br

Humberto Cardoso
FIBRAFORTE Engenharia Ind. Com. Ltda
humberto.cardoso@fibraforte.com.br

Abstract. *This work presents a thermo-elastic analysis performed through the finite element method (FEM) by means of the Nastran® software of the 5N Thruster developed by Fibraforte for the Brazilian Space Agency. The objective of the analysis is to foresee possible areas of stress concentration due to temperature gradients to wich it will be submitted during its operation causing possible crack or imperfection formations at the welding regions. The data referring to the temperature distribution are gotten by means of the SATER100® software,that uses the hybrid method of control volumes and finite elements (CVFEM), preventing compatibility problems of meshes found in most of the commercial softwares that adopt the method of finite differences.*

Keywords*: thermo-elastic analysis, thruster, finite element method, control volume method.*

1. Introduction

The function of the Propulsion Subsystem is to provide the necessary impulse for orbital maneuvers of space platforms, satellites, interplanetary vehicles, etc., after the separation of the launch vehicle. Besides, the subsystem should unsaturate the reaction wheels during the spacecraft time of life when in orbit and should also correct its attitude in the contingency mode. The subsystem is designed according to military specifications for pressurized space systems and to withstand one year and a half in integration and tests, three years in storage and launching and four years of mission in orbit.

The considered Subsystem is a monopropellant type, utilizing hydrazine (N_2H_4) from a blow-down system pressurized with gaseous Nitrogen (N_2). The impulse is produced by six 5N thruster installed in a 1m x 1m base plate. The hydrazine decomposes exothermally inside the 5N thruster catalytic chamber and the produced hot gases are accelerated and expulsed through the convergent-divergent nozzle.

2. Thruster Model

Each thruster can be divided in two main units: flow control valve and the engine. Figure 1 presents the illustrative thruster sketch, as well as its functional characteristics, and Figure 2 shows a photo of assembled thruster.

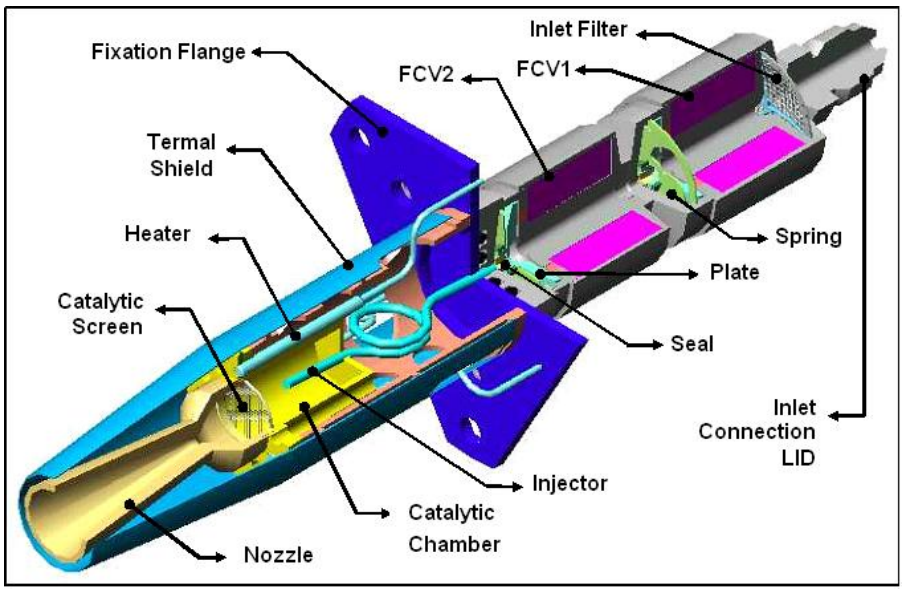

Figure 1. – Thruster Description

The flow control valve is equipped with two normally closed seals in series, in order to minimize leakage and to prevent opened failure. The magnetic circuits are made of magnetic stainless steel AISI430 with two independent coils. The opening and closing duration time are defined by the spring pre-tension and the spring course. The flow control valve incorporates a filter in the entrance and the nominal consumption is of 8W per valve.

In the engine, a calibrated injector generates a spray of propellant in the combustion chamber, where the catalytic decomposition occurs. A convergent/divergent nozzle speeds up the gases in the adequate direction. The engine is made of Inconel 600 and uses a Iridium/Alumina catalytic bed. In order to prevent the degradation of the catalyser in cold starts, each engine incorporates a heater to preheat the catalytic bed to the minimum temperature of 120^{o}C. Thermal shields block the thermal radiation for adjacent areas of the satellite.

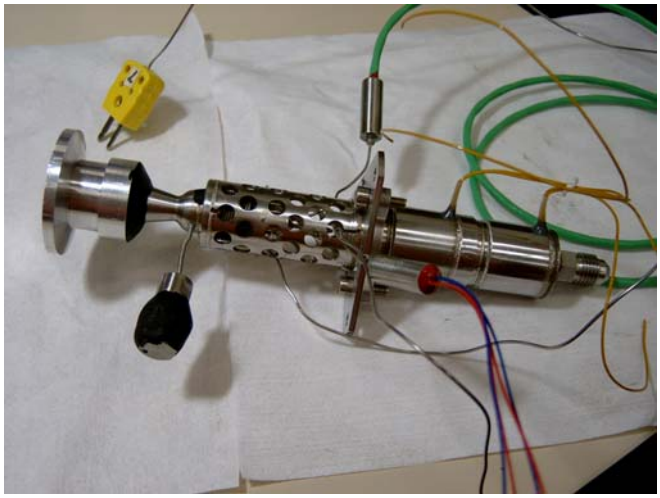

Figure 2. Assembled Thruster

3. Finite Element Model

The MSC/Nastran® software was used in association with the to FEMAP® program for the construction of the finite element model (Segerlind, 1976) and to analyze the results. The model implemented for the thruster has 32067 elements, being 31316 solid elements, 744 plate elements and 7 rigid elements and 41173 nodes, as Figure 3 shows. The total mass of the implemented model was of 0.2504 kg.

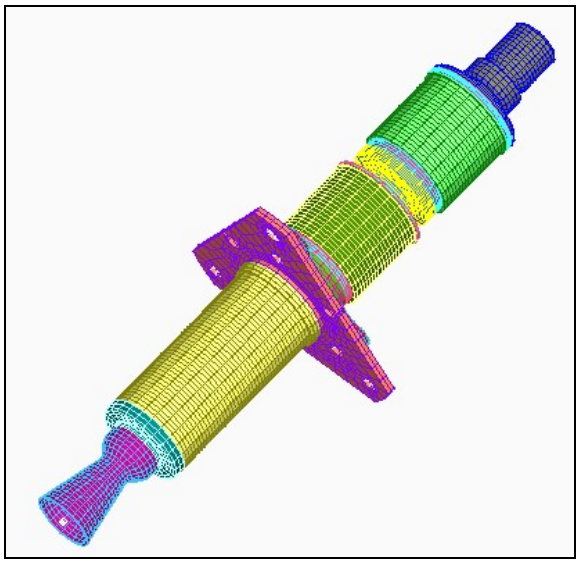

Figure 3. 5N Thruster Finite Element Model

Initially, the model consistency was verified with free-free model modes analysis, verifying the six rigid body modes. After this evaluation it was possible to proceed the thermo-elastic analysis.

4. Thermo-elastic Analysis

To perform the thermo-elastic analysis it is necessary to have: the thruster temperature distribution available in the finite element model nodes, the chamber pressure and the definition of the boundary condition as shown in Figure 4.

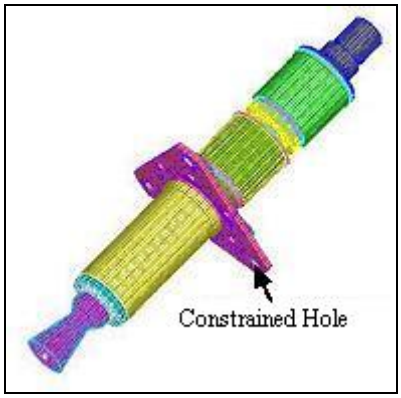

Figure 4. Definition of the Boundary Condition.

4.1. Temperature Distribution

The Nastran® requires the thruster temperature distribution to be supplied in the nodes or elements of the adopted mesh. It occurs that, normally, the thermal simulation softwares use the finite difference method in the calculation of the temperature distribution. As in this method the temperatures are calculated in finite regions, and not in the nodes, and use meshes very much coarser, consequently it becomes necessary the conversion of these data for the mesh of finite elements, that usually introduces errors in the modeling (Teichert, 1996).

The difference of the mesh refinement level is corrected easily by simple interpolations, however due to the temperature physical meaning difference, obtained by finite differences, the data convertion is more complex and laborious. In this task the geometric configuration of each region must be taken into account. The structural mesh elements which overlap each of these regions must be identified and finally, balance criteria to determinate the temperature distribution must be defined.

To overcome this difficulty, it was used here the temperature distribution generated by the Sater100® software that uses the hybrid method of control volumes and finite elements. This method consists of using the method of control volumes applied to a domain discretized similarly to the finite elements method (Cordazzo, 2005), which allows the attainment of the temperatures directly in the nodes. Figures 5 and 6 present the mesh adopted in the thermal model and the field of temperatures obtained by the SATER100®.

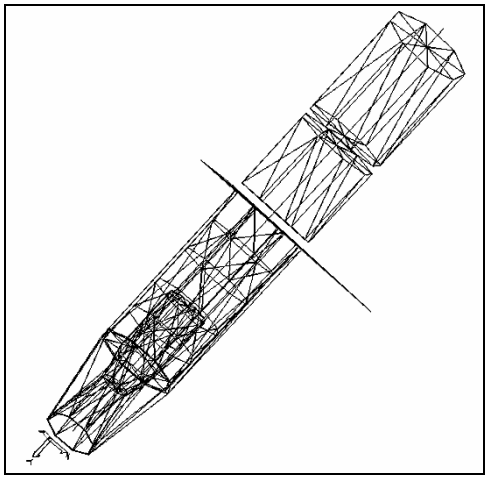

Figure. 5 – Thermal Model Adopted Mesh

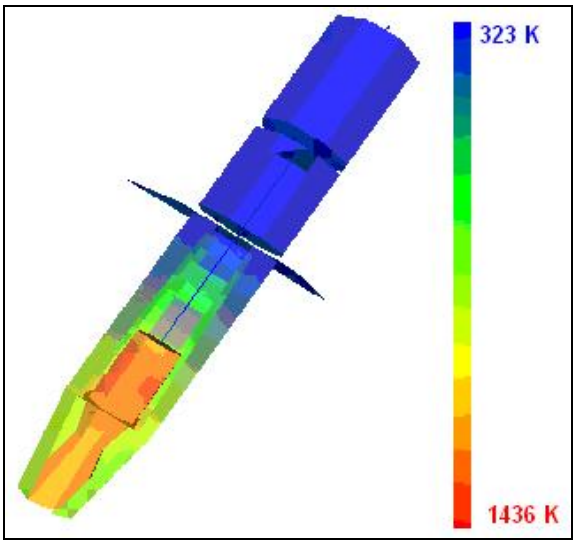

Figure. 6 – Temperature Distribution Obtained by CVFEM (SATER100®)

Then, it remained only the necessity of interpolating the values of temperature due to the difference in the refinement level of the meshes used in both models. With a lower order of magnitude, as usual, the thermal mesh presents a smaller number of nodes than the structural one. In the longitudinal direction the linear interpolation was used while that in the radial direction it was used the logarithmic interpolation, as the Eq. (1).

$$T = a \cdot \ln(r) + b \tag{1}$$

Where:

$$a = \frac{T_i - T_e}{\ln\left(r_i / r_e\right)} \tag{2}$$

$$b = T_i - a \cdot \ln(r_i) \tag{3}$$

T_i = Internal Temperature

T_e = External Temperature

r_i = Internal Radius

r_e = External Radius

r = Nodal Radius

5. Safety Margin of Welding Parts

The analyzed welding regions are shown in Fig. (7), the assignment of the components of each region is shown in Tab. 1 and the definition of the welding regions is shown in Tab. 2.

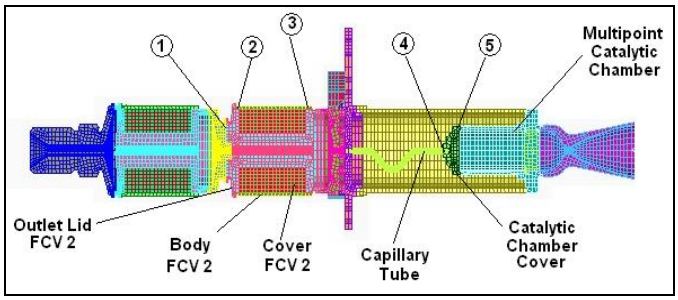

Figure 7. Component Material and Definition Assignment of the Welding Regions

Table 1. Assignment of the Thruster component materials.

COMPONENT DESIGNATION	MATERIAL
Body FCV 2	AISI 430
Cover FCV 2	AISI 430
Outlet LID 2	AISI 304
Capillary Tube	Inconel 600
Catalytic Chamber Cover	Inconel 600
Multipoint Catalytic Chamber	Inconel 600

Table 2. Critical welding parts.

Region	Critical Welding Parts
1	Outlet LID 2 with Body FCV 2
2	Superior part of Cover FCV 2 with Body FCV 2
3	Inferior part of Cover FCV 2 with Body FCV 2
4	Capilary Tube with Catalytic Chamber Cover
5	Catalytic Chamber Cover with Catalytic Chamber

To calculate the safety margins of the welding regions, it was used the Eq. (4) considering the results obtained through the term-elastic analysis of the finite element model.

$$MS = \left(\frac{\sigma_y}{Maximum\,stress \cdot Factor\,of\ safety \cdot Welding\,additional\,FS} \right) - 1 \tag{4}$$

The smaller value of σ_y is considered for calculation when it involves two or more materials. The adopted security factor is equal to 1.2 and the additional weld factor is equal to 1.5. The results of the analyses are shown in Fig. (8) to (12) with the corresponding safety margin values.

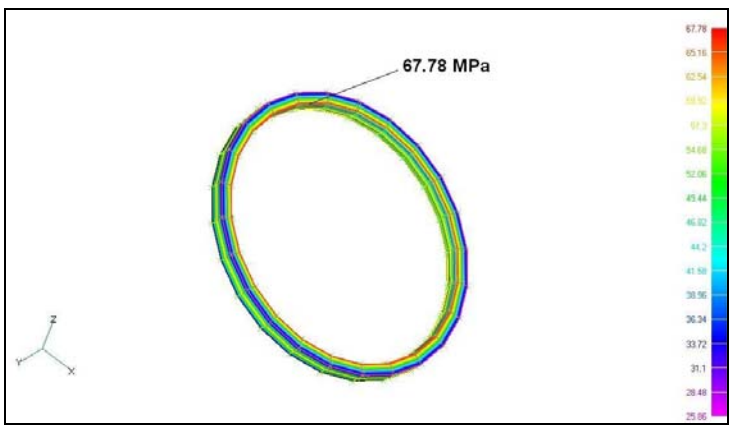

Figure 8. Welding region 1

The temperature in the considered region is equal to 92ºC and the value of the calculated MS was 83.5

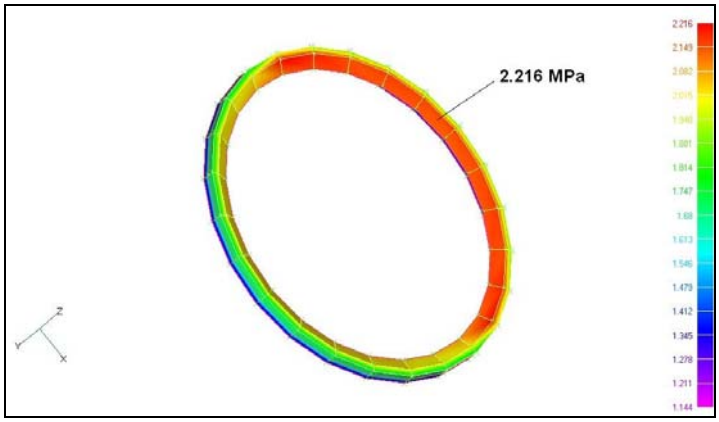

Figure 9. Welding region 2.

The temperature in the considered region is equal to 92ºC and the value of the calculated MS was 9.82.

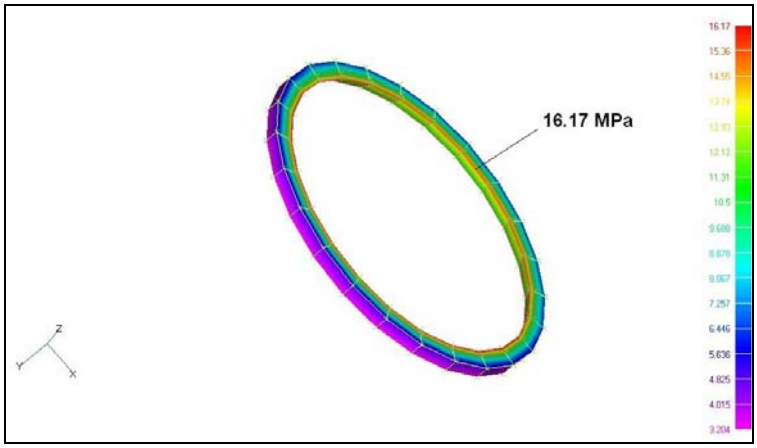

Figure 10. Welding region 3.

The temperature in the considered region is equal to 92ºC and the value of the calculated MS was 8.20.

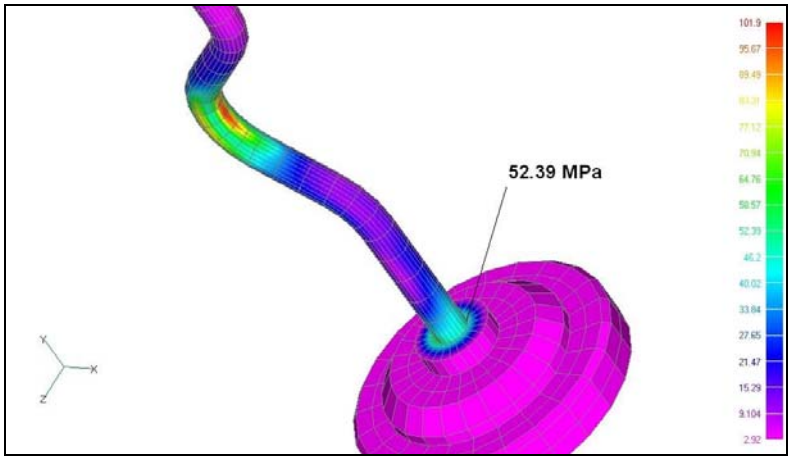

Figure 11. Welding region 4.

The temperature in the considered region is equal to 203ºC and the value of the calculated MS was 1.85.

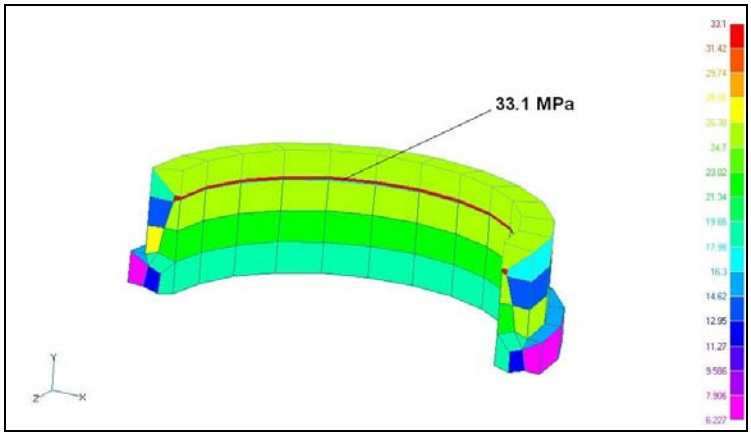

Figure 12. Welding region 5.

The temperature in the considered region is equal to 755.8ºC and the value of the calculated MS was 5.41.

2.3. Conclusion

The calculated safety margins resulted in positive values guaranteeing that the stress concentration in the welding regions will not cause disruption or crack. The most critical region is the junction between the capillary pipe and the injector (Region 4) that has presented the smaller MS (1.85). The use of the data generated by Sater100 allowed the direct application of thermal data in the finite elements mesh, avoiding the use of any conversion tool.

3. Acknowledgements

The authors wish to thank to FAPESP (Fundação de Amparo à Pesquisa do Estado de São Paulo) for the support provided for the current research.

4. References

Cordazzo, J., Maliska, C. R., 2005, "Porosity and Permeability Determination in Petroleum Reservoir Simulation Methods Using Unstructured Grids", Proceedings of 4th International Conference on Computational Heat and Mass Transfer, Paris-Cachan, France, pp.1-6.

Segerlind, L.J., 1976, "Applied Finite Element Analysis", Ed. John Wiley & Sons, New York, USA, 422 p.

Teichert, W., Klein, M., 1996, "Thermo-Elastic Analysis of Spacecraft Structures", ESA Newsletters, Preparing for the Future, Vol.6, No. 3.

5. Responsibility notice

The authors are the only responsible for the printed material included in this paper.